Surface states and reconstruction of epitaxial $\sqrt{3}\times\sqrt{3}R\,30°$ Er silicide on Si(111)

P. Wetzel, S. Saintenoy, C. Pirri, D. Bolmont, and G. Gewinner
Laboratoire de Physique et de Spectroscopie Electronique, Faculté des Sciences et Techniques, 4 rue des Frères Lumière, 68093 Mulhouse Cedex, France
(Received 2 May 1994; revised manuscript received 11 July 1994)

The surface electronic structure of epitaxial $\sqrt{3}\times\sqrt{3}R\,30°$ $ErSi_{1.7}$ layers on Si(111) has been studied by high-resolution angle-resolved ultraviolet photoemission spectroscopy. Typical surface states or resonances are unambiguously identified and their band dispersions mapped along the high-symmetry $\bar{\Gamma}\,\bar{M}$, $\bar{\Gamma}\,\bar{K}$, and $\bar{K}\,\bar{M}$ lines of the (1×1) surface Brillouin zone. These data are compared to the band structure of two-dimensional $p(1\times1)$ Er silicide extensively studied in previous works. It is found that the prominent surface bands observed in the 0–3-eV binding-energy range can be readily derived from the $p(1\times1)$ surface-silicide bands folded back into the reduced $\sqrt{3}\times\sqrt{3}$ zone. This indicates that the bulk silicide is also terminated with a buckled Si layer without vacancies, quite similar to the surface-silicide termination. In particular, specific surface bands reflect the doubly (essentially) occupied dangling bonds and the back bonds of the buckled Si top layer.

I. INTRODUCTION

Investigation of the electronic structure by angle-resolved ultraviolet photoemission spectroscopy (ARUPS) continues to be an active field of research. One of the goals of such efforts is an accurate characterization of the electronic structure of the surface which is different from that of the bulk. This means that there are electronic states, different from the bulk ones, which are confined to the surface. Therefore, these states, called surface or resonance states, are of fundamental importance in determining a large variety of microscopic and macroscopic phenomena such as surface chemical reactivity, surface reconstructions, surface magnetic order, surface energy, adhesion forces, etc.[1]

In this paper, we report a study of erbium disilicide (0001) surfaces using ARUPS. Our choice was determined by the possibility of this silicide to form well-ordered epitaxial layers on Si(111).[2] The lattice mismatch of Er disilicides with Si(111) is -1.22%. They also form with *n*-type Si a remarkably low Schottky barrier height ($\sim$0.3 eV).[3] Erbium disilicide crystallizes in the AlB_2-type lattice structure with the primitive cell parameters $c=4.09$ Å and $a=3.782$ Å. This structure is made of alternate hexagonal Er planes and graphitelike Si planes parallel to the substrate surface, but with vacancies present on the Si sublattice. It is believed that one silicon atom out of six is missing in the Si planes relative to the ideal AlB_2 structure, leading to a stoichiometry close to $ErSi_{1.7}$. Surface-extended x-ray-absorption fine-structure experiments on thick epitaxial $ErSi_{1.7}$ silicides[4] clearly indicate the relaxation of the silicon sublattice, where the Si atoms are moved from their location in the ideal AlB_2 structure, as expected by the presence of Si vacancies. Previous transmission electron diffraction and low-energy electron diffraction (LEED) analysis[5,2] attributed the appearance of superlattice diffraction spots to the formation of a $\sqrt{3}\times\sqrt{3}R\,30°$ ordered vacancy mesh, but this is not firmly established. The vacancy ordering along the surface normal [0001] axis is not well understood either. Different orderings of Si planes have been evoked. One corresponds to a stacking of vacancies on top of each other,[6] and the other is obtained by rotating one plane out of two by 120° around the [0001] axis.[7] The lattice period along the [0001] axis is then equal to *c* and 2*c*, respectively. Recently, calculations of the electronic structure of bulk erbium silicide both in the ideal AlB_2 structure ($ErSi_2$) and in the experimental one ($ErSi_{1.7}$) have been performed by empirical extended Hückel method[8] and by the linear-muffin-tin-orbital combined with tight-binding methods.[9] A comparison was made with experimental photoemission data, and better agreement was found by assuming the crystal periodicity along the [0001] axis to be 2*c*.[8] Investigations of the electronic structure of $\sqrt{3}\times\sqrt{3}R\,30°$ $ErSi_{1.7}$ by means of ARUPS experiments have been reported previously.[10,11] The angle-resolved spectra exhibit a fairly rich structure with a number of strongly dispersing features, which are sometimes as narrow as 200–300-meV full width at half maximum (FWHM). While some surface states have been identified, many spectral features could not clearly be assigned to either surface or bulk electronic states, and little information about their origin has been obtained up to now.

Here we present more accurate data about the surface electronic structure of clean $\sqrt{3}\times\sqrt{3}R\,30°$ $ErSi_{1.7}$ by high-energy and high-angular-resolution UPS. This part of our study is aimed at a better understanding of the very interesting photoemission spectra observed on epitaxial Er disilicides. Here we concentrate on the surface electronic structure of relatively thick layers ($\geq$40 Å). The bulk electronic structure as well as thin-film effects observed in ultrathin layers will be addressed elsewhere. By means of specific experiments, we have unambiguously identified a series of well-defined dispersion surface bands which can be readily followed along the $\bar{\Gamma}\,\bar{M}$, $\bar{\Gamma}\,\bar{K}$,

and $\bar{K}\,\bar{M}$ symmetry lines of the 1×1 surface Brillouin zone (SBZ). A comparison is made with the surface band structure recorded on a two-dimensional $p(1\times1)$ Er silicide,[12] and it is shown that the origin of $\sqrt{3}\times\sqrt{3}R30°$ $ErSi_{1.7}$ surface bands can be explained in terms of band folding induced by the $\sqrt{3}\times\sqrt{3}$ supercell crystal potential induced by the underlying silicide layers. This analysis strongly supports the view that the $\sqrt{3}\times\sqrt{3}R30°$ $ErSi_{1.7}$ surface termination must be essentially the same as for the two-dimensional silicide; namely, a buckled Si double layer *without vacancies*. Thus the prominent surface bands located in the 0-3-eV binding energy reflect mainly the electronic structure of this specific surface reconstruction, in particular the almost filled dangling bonds of the Si top layer.

II. EXPERIMENTAL PROCEDURE

Experiments have been performed in two separate ultrahigh-vacuum systems with a base pressure below 2×10^{-10} mbar. One chamber was equipped with a Leybold Heraeus EA 200 electron spectrometer for angle-resolved ultraviolet photoemission spectroscopy, x-ray photoemission spectroscopy, and with low-energy electron-diffraction (LEED) optics. The photoemission spectra were recorded mainly with a He I unpolarized resonance line (21.2 eV). The photoelectrons were analyzed using a hemispherical energy analyzer (150 mm in radius) with an angular resolution of $\pm1°$ and 50-meV energy resolution and an 18-channel multidetection assembly.

In Fig. 1 we show the (1×1) surface Brillouin zone (SBZ) (solid lines) along with the reduced $\sqrt{3}\times\sqrt{3}R30°$ SBZ (dashed lines). The high-symmetry points labeled $\bar{\Gamma}$, $\bar{M}$, and $\bar{K}$ refer to the (1×1) SBZ, whereas $\bar{\Gamma}'$, $\bar{M}'$, and $\bar{K}'$ refer to the $\sqrt{3}\times\sqrt{3}R30°$ SBZ. The photoemission spectra have been acquired at various polar angles Θ along the two inequivalent $\bar{\Gamma}\,\bar{M}$ and $\bar{\Gamma}\,\bar{K}$ high-symmetry lines of the (1×1) SBZ. In this manner it is possible to map the two-dimensional band dispersion of the $\sqrt{3}\times\sqrt{3}R30°$ $ErSi_{1.7}$ surface states. The component of the photoelectrons wave vector parallel to the sample surface ($k_\parallel$) is calculated using the standard equation $k_\parallel=0.52\sqrt{E}\sin\Theta$, where E and Θ, respectively, are the kinetic energy and the angle of emission with respect to the sample normal of the photoelectrons.

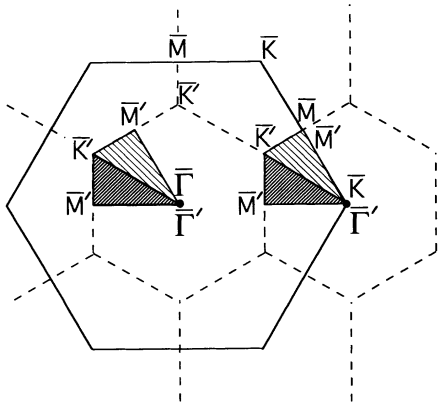

FIG. 1. Surface Brillouin zones (SBZ's) of epitaxial Er silicides. The solid and dashed lines denote the (1×1) and $\sqrt{3}\times\sqrt{3}R30°$ SBZ's respectively. The high-symmetry points labeled $\bar{\Gamma}$, $\bar{M}$, and $\bar{K}$ refer to the (1×1) SBZ, whereas the $\bar{\Gamma}'$, $\bar{M}'$, and $\bar{K}'$ refer to the $\sqrt{3}\times\sqrt{3}R30°$ SBZ. The two hatched triangle areas cover equivalent (inequivalent) parts of the $\sqrt{3}\times\sqrt{3}R30°$ (1×1) SBZ.

Sample preparations have been carried out in a second chamber containing usual facilities for surface cleaning (ion bombardment and heating), erbium and silicon evaporations, film thickness monitoring via quartz microbalances, and a quadrupole mass spectrometer. Clean Si(111) 7×7 substrate surfaces (n type) were prepared by cycles of argon-ion sputtering followed by annealing at 850 °C. Er and Si were evaporated from pyrolitic boron nitride and graphite crucibles, respectively, onto the 7×7 Si(111) surface. After prolonged degassing of the sources, we obtained stable rates of evaporation of about 1 monolayer/min. The coverage units used refer to the unrecontructed Si(111) substrate: 1 monolayer (ML) $\equiv7.8\times10^{14}$ atoms/cm^2. An 80-Å-thick $ErSi_{1.7}$ layer was prepared by codeposition of Er and Si at a rate ratio close to 1:1.7 followed by a 30-min anneal at 750 °C. This technique yields well-ordered $ErSi_{1.7}$ layers as evidenced by LEED, which shows a very sharp $\sqrt{3}\times\sqrt{3}$ pattern with sixfold rotational symmetry. Transmission electron microscopy studies[13] indicate that similarly prepared layers are quite uniform and essentially free of pinholes. The coevaporation technique avoids the transport of the Si and/or Er species over macroscopic distances during annealing, which is the most probable mechanism for defect creation. This could explain the poor morphology of the Er silicide films obtained by solid phase epitaxy, i.e., deposition of a pure Er film on the Si surface followed by annealing.[2]

III. RESULTS AND DISCUSSION

Figures 2 and 3 show how the photoemission spectra measured on a clean 80-Å-thick epitaxial $ErSi_{1.7}$ silicide film evolve, as a function of subsequent Si deposit. They were recorded with He I photon energy at two high-symmetry points of the (1×1) SBZ, namely the $\bar{\Gamma}$ and $\bar{M}$ points. In both figures the bottom curve corresponds to the clean $ErSi_{1.7}$ surface. At the $\bar{\Gamma}$ point (Fig. 2), we note the presence of six structures labeled, from lower to higher binding energy (BE), A (0.36 eV), B (0.85 eV), C (1.30 eV), D (1.80 eV), E (2.30 eV), and F (2.85 eV). The spectrum is essentially dominated by two particularly narrow emission peaks (FWHM = 300 meV) labeled D and E, and a broader structured peak centered at ~1.00-eV BE. This broad structure shows a more pronounced sharp feature at 0.85-eV BE (B). Finally, a peak (A) appears close to the Fermi level. At the $\bar{M}$ point (Fig. 3), the spectra exhibit a conspicuous double-peaked structure close to the Fermi level and located at ~0.22- and ~0.44-eV BE, respectively. At higher BE's features are visible at ~1.00- and 1.85-eV BE together with shoulders at 1.60- and 2.30-eV BE. Finally, a broad and strong structure appears at 2.80-eV BE. These features

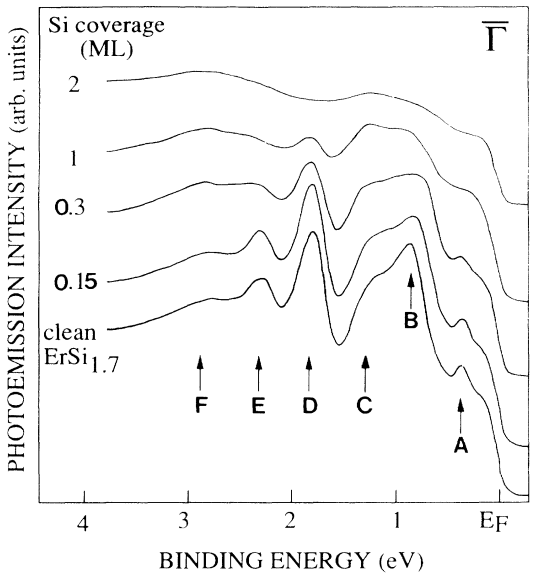

FIG. 2. Evolution of the ARUPS spectra measured on an 80-Å-thick epitaxial $ErSi_{1.7}$ silicide layer, as a function of subsequent Si deposit. They are recorded with He I radiations at the $\bar{\Gamma}$ point. Si is deposited on the bulklike Er silicide surface kept at room temperature.

are labeled, from lower to higher BE, *G* (0.22 eV), *H* (0.44 eV), *I* (1.00 eV), *J* (1.60 eV), *K* (1.86 eV), *L* (2.30 eV), and *M* (2.80 eV).

A main point in spectral analysis is to distinguish unambiguously between bulk and surface emission among all these spectral features. This is particularly important in photoemission from compounds with reconstructed surfaces, where the surface electronic structure dominates the spectrum, as happens to be the case of $ErSi_{1.7}$ (0001). A usual test is based on the chemisorption of various species on the surface and following the changes

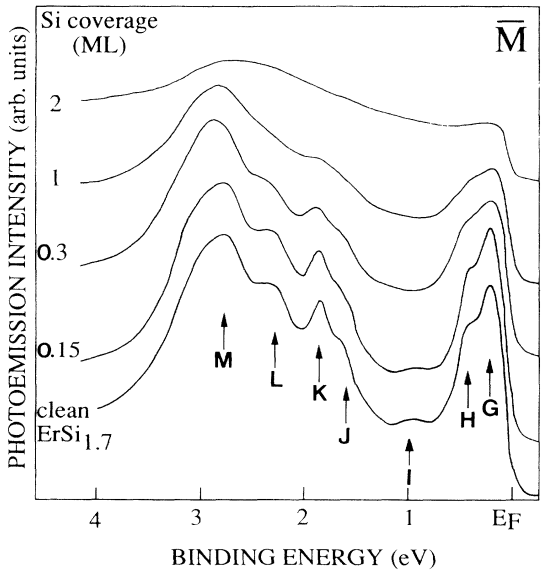

FIG 3. Same as Fig. 2, but the spectra are recorded at the $\bar{M}$ point.

brought about in the ARUPS spectra. Emission originating from the surface-localized bands is expected to be particularly sensitive to the modification of the surface since this changes the surface electronic structure, so that the photoemission feature will be quenched and/or shifted in binding energy. Because of inelastic and elastic scattering of the photoelectrons in the chemisorbed layer, the bulk peaks are also attenuated, but the attenuation is very progressive and complete quenching is not expected by chemisorption in the monolayer range. In the present case, O_2 adsorption has been used previously,[8,14] but the relatively inert character of the Er silicide surfaces needs very large exposures. Here we use a different approach where small amounts of Si or Er are deposited at room temperature by evaporation. This results in disordered chemisorption of these species with a sticking coefficient close to 1. In this way a more refined study of the behavior of the various spectral features upon chemisorption of very small well-controlled amounts of adsorbates can be achieved. It can be seen in Fig. 2 that peak *B*, located at 0.85-eV BE, decreases in intensity for a Si deposit as small as 0.15 ML, while the other structures, including those observed at the $\bar{M}$ point (Fig. 3), are almost unaffected. Further Si dosing results in the quenching of peak *B* for a Si deposit of 0.3 ML, and in a rapid decrease in intensity of the *D* and *E* (*G*, *H*, *I*, *J*, *K*, *L*, and *M*) features at $\bar{\Gamma}$ ($\bar{M}$). These peaks, except for *H* and *G* close to the Fermi level, at $\bar{M}$ are almost completely removed for a 1-ML Si deposit. Further deposition of ~1 ML of Si also completely removes the prominent *G* and *H* peaks at $\bar{M}$. At this stage, only two broad structures centered at ~1.30 and ~2.85-eV BE remain visible at $\bar{\Gamma}$. Similarly at $\bar{M}$ only the structure at 2.8 eV is left. In view of the small quantity of Si deposited, it is quite clear that the completely quenched features have to be assigned to surface-state or resonance emissions. In contrast, the peaks still visible at this stage are most likely related to bulk emission and will be discussed in more detail elsewhere.[15] Thus the chemisorption experiments clearly indicate that the surface state at 0.85 eV is superimposed on bulk components. Theoretical calculations[8] also show that peak *A*, though more sensitive to chemisorption, is also related to the bulk band structure.

The surface character of the electron states associated with the *B*, *D*, *E*, *G*, *H I*, *J*, *K*, and *L* peaks can be further asserted upon Er deposit at room temperature. Figure 4 shows the evolution of the spectrum at $\bar{\Gamma}$ as a function of Er deposit. It can be seen that features *D* and *E* become practically undetectable for a total Er dose as small as 0.2 ML. In contrast, the shape of the broad structure centered at 1.00-eV BE remains the same as a function of Er coverage. It is also interesting to note that the peak labeled *B* is almost unaffected after deposition of 0.2 ML of Er, in contrast to both *D* and *E* features which are almost fully removed. This contrasts with the behavior observed upon Si deposition, since it was found that 0.3 ML of Si quenched the *B* but not the *D* and *E* peaks. From these experiments, it is apparent that the surface state labeled *B* has a definitely different character when compared to the other ones. This suggests that initially the adsorption sites for Er and Si atoms on clean $ErSi_{1.7}$ surfaces are

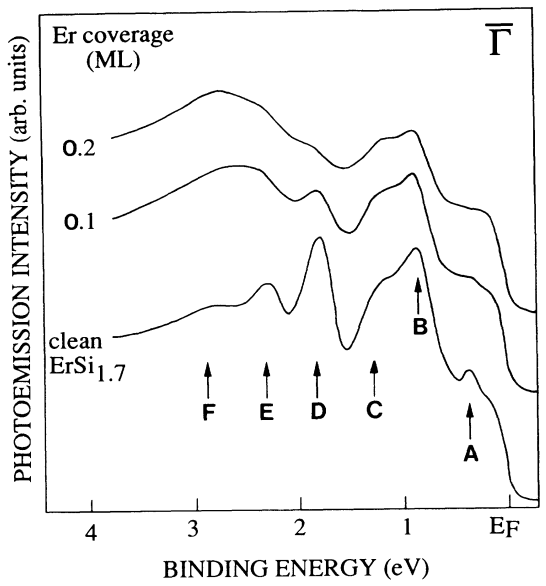

FIG. 4. Same as Fig. 2, but the ARUPS spectra are measured as a function of subsequent Er deposit.

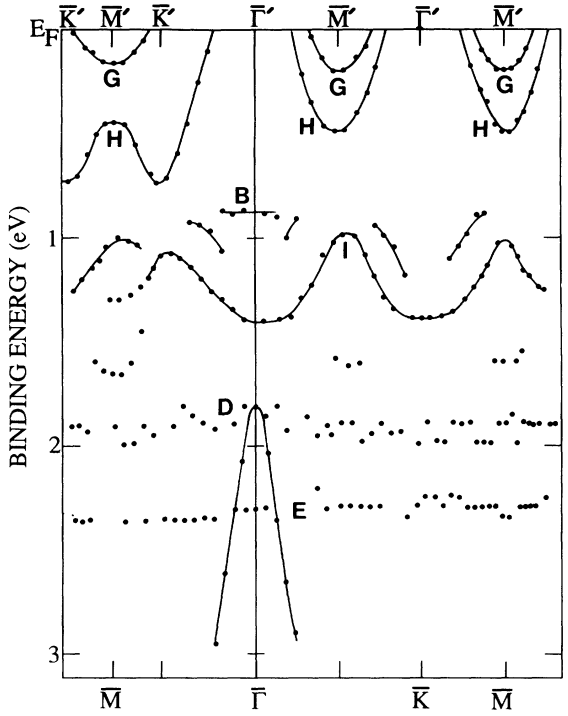

FIG. 5. The dispersion of the surface bands measured on the $\sqrt{3}\times\sqrt{3}R30°$ $ErSi_{1.7}$ silicide surface along the $\bar{\Gamma}\bar{M}$, $\bar{\Gamma}\bar{K}$, and $\bar{K}\bar{M}$ symmetry lines of the (1×1) SBZ. The letter symbols are those used in Figs. 2–4. The solid dots denote the experimental data collected with He I photon energy. The solid lines are guides to the eye to illustrate the band dispersions.

different and correspond to the specific localization of the relevant surface states in real space. For instance, one would expect that Er tends to bind to Si sites, so that the *D* and *E* features should be localized on these sites, in contrast to feature *B* which is localized on Er sites.

Previous experiments[8,14] have shown that at $\bar{\Gamma}$ the peaks located at 1.80, 2.30, and 0.85 eV below the Fermi level are very sensitive to oxygen adsorption and that no energy dispersion is observed with respect to the momentum component normal to the surface. In contrast, the broad feature centered at 1.00-eV BE is much less affected by oxygen exposure. These observations agree with the present interpretation in terms of surface states.

In the same way, we have systematically investigated the surface versus bulk character of the various spectral features in off-normal spectra by means of Er and Si deposit experiments. The energy dispersion, along the $\bar{\Gamma}\bar{M}$, $\bar{\Gamma}\bar{K}$, and $\bar{K}\bar{M}$ high-symmetry directions, of the various surface features identified in this way on clean $\sqrt{3}\times\sqrt{3}R30°$ $ErSi_{1.7}$ are plotted versus the parallel momentum $k_{\parallel}$ of the photoelectrons in Fig. 5. We have kept the labels used for the surface states (Figs. 2–4) in order to identify the various surface bands. The data in this figure include results obtained in the 0–3-eV BE range. We have also checked that these bands satisfy the basic criterion for a surface band, namely that their binding energies measured for a given $k_{\parallel}$ are the same for Ne I, He I, and He II photons. In this respect we note that generally the spectral features, even the bulk-related ones, show little or no dispersion versus the photon energy or perpendicular component of the momentum. This observation stresses the importance of careful chemisorption experiments for the interpretation of the spectra. As can be seen in Fig. 5, the dispersion of all surface bands clearly shows the symmetry of the $\sqrt{3}\times\sqrt{3}$ $R30°$ SBZ. Note in particular the periodicity and extremal behavior at the equivalent $\bar{M}$ and $\bar{M}'$ points of the $\sqrt{3}\times\sqrt{3}R30°$ SBZ and at the equivalent $\bar{\Gamma}'$ and $\bar{K}$ points of the $\sqrt{3}\times\sqrt{3}R30°$ SBZ and 1×1 SBZ, respectively.

Along the $\bar{\Gamma}\bar{K}$ azimuth, two surface bands (*G* and *H*) which have maximum BE's of 0.2 and 0.5 eV, respectively, show symmetric dispersion about the equivalent points $\bar{M}$ and $\bar{M}'$ of the $\sqrt{3}\times\sqrt{3}R30°$ SBZ. These bands crossing the Fermi level clearly indicate the metallic character of the surface. A third surface band related to feature *I* at $\bar{\Gamma}$ nicely shows the periodicity of the $\sqrt{3}\times\sqrt{3}R30°$ SBZ. This band has a maximum BE of 1.40 eV at $\bar{\Gamma}$ and $\bar{K}$ points, and a minimum BE of ~1.00 eV at $\bar{M}$ and $\bar{M}'$ points. Close to $\bar{\Gamma}$ the structure *I* shows low emission intensity, while for off-normal emission its intensity increases drastically and reaches a maximum at $\bar{K}$. At $\bar{\Gamma}$, we see that two bands are related to the surface or resonance peak *D* located at 1.80-eV BE. One band remains quite flat over the whole $\sqrt{3}\times\sqrt{3}R30°$ SBZ while the other one disperses very strongly toward higher BE's. Finally, the highest BE surface band (*E*) also shows little dispersion over the whole $\sqrt{3}\times\sqrt{3}R30°$ SBZ.

Along the $\bar{\Gamma}\bar{M}$ azimuth, surface bands *G* and *H* show similar dispersions about the $\bar{M}'$ ($\bar{M}$) point. The former, which has a maximum BE of 0.20 eV, disperses upwards when moving toward $\bar{K}'$ and crosses the Fermi level. The second has a BE of 0.5 eV at $\bar{M}'$ ($\bar{M}$). It disperses away from the Fermi level, reaches its maximum BE at 0.7 eV, then reverses direction and crosses the Fermi level around $\bar{\Gamma}$. We observe another band which has a max-

imum BE of 1.40 eV at the $\bar{\Gamma}$ point and a minimum BE at the $\bar{K}'$ or $\bar{M}'$ points. Concerning the surface state B located at 0.85-eV BE, it is observable only around the $\bar{\Gamma}$ point and shows no dispersion.

Having clearly identified a complete set of $\sqrt{3}\times\sqrt{3}R30°$ $ErSi_{1.7}$ surface bands, we now demonstrate that the origin of the major bands can be understood in a physically transparent way when considering previous works. In this respect it has been shown that a well-ordered single layer of Er silicide with $ErSi_2$ stoichiometry and $p(1\times1)$ symmetry can be prepared by depositing one Er monolayer and annealing at 400 °C.[12,16,17] This silicide has the same $p3m1$ symmetry as the Si(111) surface, and only a single domain is actually formed. A complete description of the atomic structure of this two-dimensional (2D) epitaxial silicide has been obtained by combining Auger electron diffraction and surface-extended x-ray-absorption fine structure.[18] The atomic arrangement consists of a hexagonal Er monolayer underneath a buckled Si top layer, as depicted in Fig. 6. The Er atom resides at the T_4 position, i.e., occupies eclipsed threefold hollow sites of the Si(111) substrate termination, and the top Si double layer is rotated by 180° around the surface normal with respect to the substrate. Moreover, a photoelectron diffraction analysis[16] shows that bulklike Er silicide films exhibit a reconstructed surface termination probably similar to the 2D Er silicide surface termination, made of a buckled Si double layer. It is thus of a great interest to compare the $\sqrt{3}\times\sqrt{3}R30°$ $ErSi_{1.7}$ related surface bands to the $p(1\times1)$ 2D Er silicide ones.

The band dispersions for $p(1\times1)$ 2D silicide, along the $\bar{\Gamma}\bar{M}$, $\bar{\Gamma}\bar{K}$, and $\bar{K}\bar{M}$ symmetry lines, inferred from high-resolution photoemission experiments[12] are shown in Fig. 7. One prominent surface band corresponds to a nearly filled band that crosses the Fermi level near $\bar{\Gamma}$ and has a maximum BE at 1.65 eV near $\bar{M}$. The other one is a nearly empty band with a BE of $\sim$0.10 eV at $\bar{M}$. It disperses symmetrically around the $\bar{M}$ point and crosses

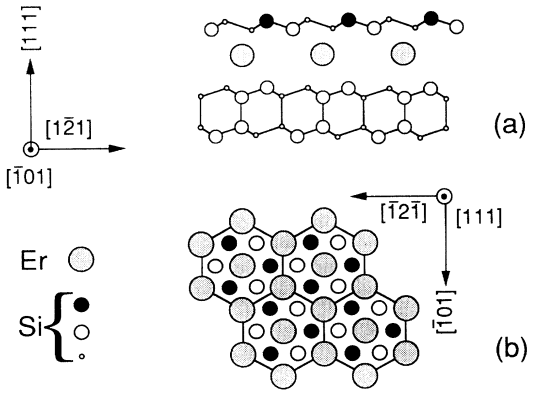

FIG. 6. (a) A sketch of the atomic structure of the $ErSi_2$ surface silicide projected along the [$\bar{1}$01] direction. (b) A top view of the same structure. Large solid circles refer to the Er atoms, and small solid circles to the Si top layer atoms. In (a) the large and small open circles represent Si atoms in the plane of the paper, and in the ($\bar{1}$01) plane immediately above the paper, respectively.

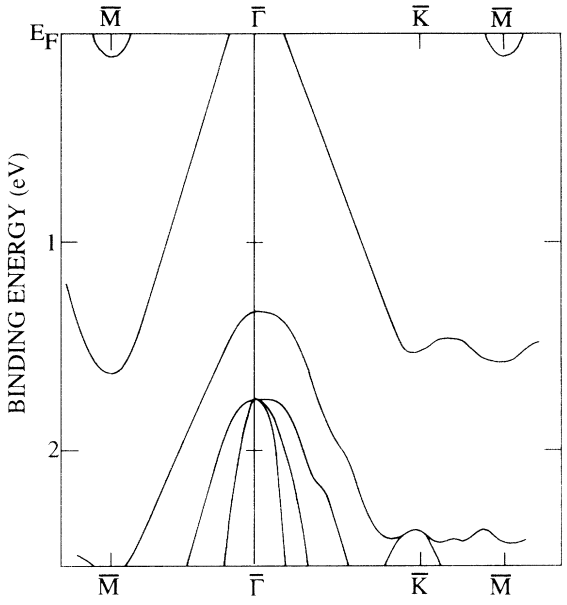

FIG. 7. Experimental band dispersions obtained along the $\bar{\Gamma}\bar{M}$, $\bar{\Gamma}\bar{K}$, and $\bar{K}\bar{M}$ symmetry lines for the two-dimensional Er silicide (Ref. 12). The data were collected with He I photon energy.

the Fermi level near $\bar{M}$. In conjunction with band-structure calculations by means of the crystalline extension of the extended Hückel method[19] it was found that the almost-empty band exhibits over the whole SBZ strong hybridization between Er $5d$ states and Si $3p$ states from the Si double layer just above and just below the Er plane. The almost-filled band has a similar character at $\bar{\Gamma}$. Off $\bar{\Gamma}$, this band acquires progressively dominant Si $3p_z$ character and mainly derives from dangling bonds of the topmost Si double layer. Finally, the 2D Fermi surface of this silicide, which consists of a small hole pocket at $\bar{\Gamma}$ and small electron pocket at $\bar{M}$, is typical of a semimetal.

It can be seen from Figs. 5 and 7 that the surface band dispersions for bulklike and 2D silicides display very striking similarities. Most obviously, one observes almost identical 2D Fermi surfaces with a nearly-empty band which crosses the Fermi level near $\bar{M}$, and a nearly filled band crossing the Fermi level near the $\bar{\Gamma}$ point. Only the size of the electron and hole pockets is somewhat larger for the $\sqrt{3}\times\sqrt{3}R30°$ surface. These similarities can be explained to a large extent in term of backfolding of the (1×1) bands in the reduced $\sqrt{3}\times\sqrt{3}$ zone. The bands recorded on bulk $ErSi_{1.7}$ silicide show a $\sqrt{3}\times\sqrt{3}R30°$ periodicity in contrast to the (1×1) periodicity of the 2D silicide. In a first approximation, if the surface structures are indeed similar for both silicides, the bands in the $\sqrt{3}\times\sqrt{3}$ zone should be obtained by translating the $p(1\times1)$ band states of the $\bar{M}'\bar{K}\bar{K}'$ and $\bar{K}\bar{M}\bar{K}'$ triangles in Fig. 1 into the reduced zone along $\bar{\Gamma}\bar{K}$. Therefore, bands recorded along the $\bar{K}\bar{M}'$ and $\bar{K}\bar{M}$ ($\bar{K}'\bar{M}$ and $\bar{K}'\bar{M}'$) lines are backfolded on the $\bar{\Gamma}'\bar{M}'$ ($\bar{K}'\bar{M}'$) line while two degenerated bands along the $\bar{K}\bar{K}'$ line are backfolded along the $\bar{\Gamma}'\bar{K}'$ line. Whether or not this

backfolding of the bands can be observed experimentally depends on the strength of the potential component with $\sqrt{3}\times\sqrt{3}$ periodicity and related umklapps due to the additional reciprocal-lattice vectors. This potential is related to the $\sqrt{3}\times\sqrt{3}$ superstructure of the underlying bulk silicide, and is possibly due to a periodic arrangement of vacancies in graphitelike Si planes.

Figure 8 shows the band dispersions measured on the 2D Er silicide drawn in the (1×1) (solid lines) and reduced $\sqrt{3}\times\sqrt{3}$ (the dashed bands are backfolded bands) surface Brillouin zones. Along the $\bar{\Gamma}\bar{M}$ and $\bar{\Gamma}\bar{K}$ lines band crossings occur at $\bar{K}'$ ($\sim$1.15-eV BE) and $\bar{M}'$ ($\sim$0.7-eV BE), respectively. Because of the $\sqrt{3}\times\sqrt{3}$ perturbation potential, one expects the opening of gaps at such points. A schematic sketch of the resulting bands (dotted lines) as expected from an analysis based on group theory is also presented in Fig. 8. Note that each band in the (1×1) zone results in three bands in the $\sqrt{3}\times\sqrt{3}$ zone. A comparison of Figs. 8 and 5 shows that almost all surface bands observed on bulklike $\sqrt{3}\times\sqrt{3}R\,30°$ $ErSi_{1.7}$ (0001) surface are qualitatively well predicted with respect to their topology and location by means of backfolded 2D silicide bands. In particular the surface bands labeled *G*, *H*, and *I* as well as the Fermi surface are nicely reproduced in this way when the shifts and splitting of degenerate states due to the new crystal potential are taken into account. Note also that Fig. 8 displays a strongly dispersive (nearly flat band) at $\sim$1.80-eV BE ($\sim$2.40-eV BE) near $\bar{\Gamma}$ (along the $\bar{\Gamma}\bar{K}$ line) which could be assigned to the observed *D* (*E*) surface band. Both bulk and two-dimensional Er silicide surface band structures also display a band ($\sim$1.80-eV BE) at $\bar{\Gamma}$, dispersing rapidly away from the Fermi level with increasing $k_{\parallel}$. The

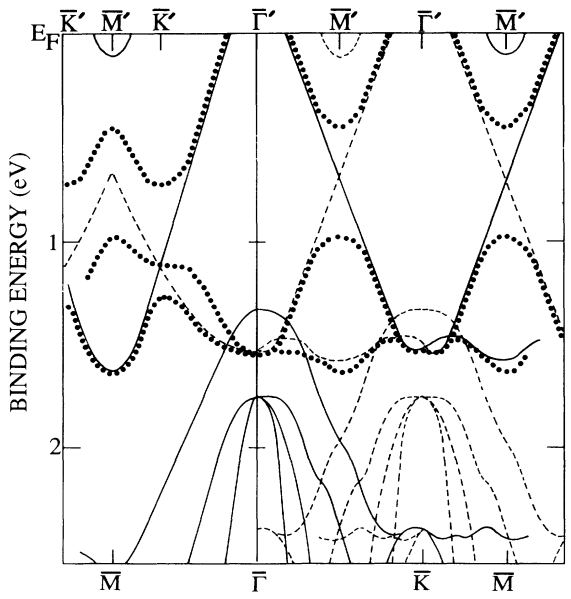

FIG. 8. Experimental band dispersions measured on the two-dimensional Er silicide drawn in the 1×1 (solid lines) and reduced $\sqrt{3}\times\sqrt{3}$ surface Brillouin zones. The dashed lines are backfolded bands, while dotted bands are obtained after opening gaps at $\bar{M}'$ and $\bar{K}'$ points and from analysis based on group theory.

present analysis indicates that major surface bands observed on $ErSi_{1.7}$(0001) have the same physical origin as the relevant (1×1) bands observed on the 2D silicide, i.e., they reflect the electronic structure of a reconstructed top layer consisting in a buckled Si layer which adopts a geometry similar to a Si(111) double layer in bulk Si. According to previous work on the $p(1\times1)$ silicide,[19] if this picture is indeed correct bands *G*, *H*, and *I* reflect dangling-bond states while band *D* corresponds to back bonds of the buckled Si top layer.

The present finding strongly suggests that the bulklike $\sqrt{3}\times\sqrt{3}R\,30°$ $ErSi_{1.7}$ silicide surface indeed has an atomic structure very similar to that of the two-dimensional silicide. When compared to the ideal Si(111) termination such a surface becomes stable for the silicide because of Er electron donation which leads to almost-filled surface dangling bonds.[12] At this stage, let us note that in the case of 2D Er silicide the buckled surface Si layer does not involve Si vacancies. So in view of the present findings there is *a priori* no reason to invoke the presence of vacancies in the reconstructed Si top layer of bulklike $ErSi_{1.7}$(0001), as sometimes suggested in previous work.[10] A physical argument which explains the expulsion of Si atoms from the hexagonal Si rings in bulk silicide, leading to vacancies, is the release of the compressive strain. In the case of the Si top layer there is no need to eject Si atoms since the surface buckling of the Si layer already results in a release of the compressive strain. Actually the observed band structure (Fig. 5) appears to be quite consistent with the relatively weak changes expected in the $p(1\times1)$ bands of the top Si double layer when the $\sqrt{3}$ periodic potential due to *the underlying bulklike silicide layers* is turned on. Obviously, the original shape of the bands is still easily recognized, and the gaps induced by the perturbing potential are fairly small ($\sim$0.5 eV at $\bar{M}'$). If vacancies were present in the top layer one would expect a very strong perturbation and much more drastic changes in the surface electronic structure. In this respect, we would like to emphasize that our experiments clearly indicate that the $\sqrt{3}\times\sqrt{3}R\,30°$ superstructure observed in LEED essentially reflects the periodic potential in bulk silicide since we find that it is not destroyed upon Si deposition in the monolayer range, which according to the surface-state behavior described above strongly perturbs the surface structure. The only effect of 1 or even 2 ML of Si deposited at room temperature is an increase in diffuse background due to incoherent scattering in the disordered top layers. However, the relative strength of the fractional order with respect to the integral order spots exhibits little change. Again, there is no need to invoke the presence of vacancies in the Si top layer in order to explain the observed LEED superstructure. In fact, a simple electron counting argument also shows that Si vacancies in the top layer are inconsistent with the observed 2D Fermi surface. For instance if one removes one Si atom out of six in the top layer there is a loss of four valence electrons per $\sqrt{3}$ unit cell. This means that the topmost backfolded surface dangling-bond-derived bands (corresponding to bands *G*, *H*, and *I* in the observed band structure) should be empty bands for bulklike $ErSi_{1.7}$, since they contain exactly four electrons in 2D silicide

without vacancies in the Si top layer. Put in another way this rigid band shift argument means that the interaction of the additional dangling bonds results in the formation of vacancy-derived states lying lower in energy than the surface dangling-bond states. Hence they act as electron acceptors and become doubly occupied. This in turn leads to empty as opposed to nearly filled surface dangling bonds and an unstable surface. Thus we conclude that the reconstructed Si double-layer termination of $ErSi_{1.7}(0001)$ does not contain periodically arranged Si vacancies. The bulklike $\sqrt{3}\times\sqrt{3}R30°$ $ErSi_{1.7}$ films exhibit a sixfold rotational symmetry as opposed to the threefold 2D Er silicide one, indicating that the two possible domains are actually formed on the bulk Er silicide surface. The buckled Si top layer can have the same orientation (type *A*), or can be rotated 180° about the surface normal (type *B*) with respect to the double layer in the bulk Si substrate.

Finally, by now, the exact nature of the surface state labeled *B* and located at 0.85-eV BE is not well understood. In contrast to the other surface states, it cannot be explained within the simple band backfolding scheme developed above, and its counterpart is not observed on the 2D Er silicide. Thus it is probably not induced by the buckled Si top layer. The particular behavior of this surface state observed on chemisorption of Er and Si atoms also supports this point of view.

In summary, we have probed the surface electronic structure of bulklike $\sqrt{3}\times\sqrt{3}R30°$ $ErSi_{1.7}$ silicide using high-resolution ARUPS in conjunction with carefully controlled chemisorption experiments. We have identified major surface bands in the 0–3-eV BE. A comparison with a two-dimensional Er silicide band structure leads to the conclusion that most observed surface bands derive from the electronic structure of a specific surface reconstruction of $ErSi_{1.7}(0001)$ which consists of a buckled Si top layer instead of the graphitelike Si termination expected for a simple truncation of the bulk structure. The observed 2D Fermi surface indicates the absence of vacancies in this reconstructed top layer.

ACKNOWLEDGMENT

The Laboratoire de Physique et de Spectroscopie Electronique is Unité Associée au CNRS No. 1435.

[1]H. Lüth, *Surfaces and Interfaces of Solid,* 2nd ed. (Springer-Verlag, Berlin, 1993).

[2]F. Arnaud d'Avitaya, A. Perio, J. C. Oberlin, Y. Campidelli, and J. A. Chroboczeck, Appl. Phys. Lett. **54**, 2198 (1989).

[3]J. Y. Duboz, P. A. Badoz, A. Perio, J. C. Oberlin, F. Arnaud d'Avitaya, Y. Campidelli, and J. A. Chroboczeck, Appl. Surf. Sci. **38**, 171 (1989).

[4]M. H. Tuilier, C. Pirri, P. Wetzel, G. Gewinner, J. Y. Veuillen, and T. A. Nguyen Tan, Surf. Sci. **307-309**, 710 (1994).

[5]J. A. Knapp and S. T. Picraux, in *Thin Films—Interfaces and Phenomena,* edited by R. J. Nemanich, P. S. Ho, and S. S. Lau, MRS Symposia Proceedings No. 54 (Materials Research Society, Pittsburgh, 1986), p. 261.

[6]A. Iandelli, A. Palenzona, and G. L. Oliesi, J. Less-Common. Metals **64**, 213 (1979).

[7]R. Baptist, S. Ferrer, G. Grenet, and H. C. Poon, Phys. Rev. Lett. **64**, 313 (1990).

[8]L. Stauffer, C. Pirri, P. Wetzel, A. Mharchi, P. Paki, D. Bolmont, G. Gewinner, and C. Minot, Phys. Rev. B **46**, 13201 (1992).

[9]G. Allan, I. Lefebvre, and N. E. Christensen, Phys. Rev. **48**, 8572 (1993).

[10]J. Y. Veuillen, T. A. Nguyen Tan, and D. B. B. Lollman, Surf. Sci. **293**, 86 (1993).

[11]P. Paki, U. Kafader, P. Wetzel, C. Pirri, J. C. Peruchetti, D. Bolmont, and G. Gewinner, Surf. Sci. **269/270**, 970 (1992).

[12]P. Wetzel, C. Pirri, P. Paki, J. C. Peruchetti, D. Bolmont, and G. Gewinner, Solid State Commun. **82**, 235 (1992).

[13]F. H. Kaatz, W. R. Graham, and J. Van der Spiegel, Appl. Phys. Lett. **62**, 1748 (1993).

[14]J. Y. Veuillen, L. Magaud, D. B. B. Lollman, and T. A. Nguyen Tan, Surf. Sci. **269/270**, 964 (1992).

[15]S. Saintenoy, P. Wetzel, C. Pirri, J. C. Peruchetti, D. Bolmont, and G. Gewinner (unpublished).

[16]P. Paki, U. Kafader, P. Wetzel, C. Pirri, J. C. Peruchetti, D. Bolmont, and G. Gewinner, Phys. Rev. B **45**, 8490 (1992).

[17]J.-Y. Veuillen, D. B. B. Lollman, T. A. Nguyen Tan, and L. Magaud, Appl. Surf. Sci. **65/66**, 712 (1993).

[18]M. H. Tuilier, P. Wetzel, C. Pirri, D. Bolmont, and G. Gewinner, Phys. Rev. B **50**, 2333 (1994).

[19]L. Stauffer, A. Mharchi, C. Pirri, P. Wetzel, D. Bolmont, G. Gewinner, and C. Minot, Phys. Rev. B **47**, 10 555 (1993).

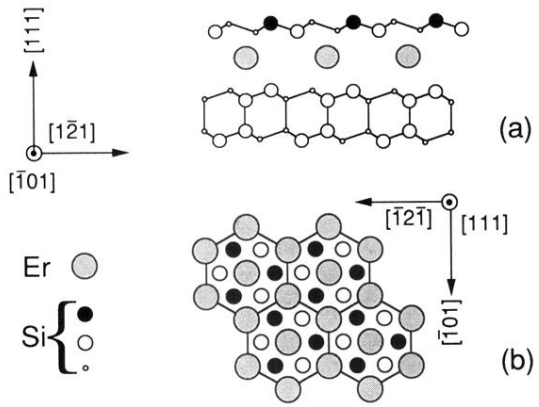

FIG. 6. (a) A sketch of the atomic structure of the $ErSi_2$ surface silicide projected along the [$\bar{1}$01] direction. (b) A top view of the same structure. Large solid circles refer to the Er atoms, and small solid circles to the Si top layer atoms. In (a) the large and small open circles represent Si atoms in the plane of the paper, and in the ($\bar{1}$01) plane immediately above the paper, respectively.